Published online 26 March 2009 *Nucleic Acids Research, 2009, Vol. 37, No. 10* ***3321–3331***
doi:10.1093/nar/gkp196

Elevated polyamines induce c-*MYC* overexpression by perturbing quadruplex–WC duplex equilibrium

Niti Kumar, Richa Basundra and Souvik Maiti*

Proteomics and Structural Biology Unit, Institute of Genomics and Integrative Biology, CSIR, Mall Road, Delhi 110 007, India

Received January 29, 2009; Revised March 8, 2009; Accepted March 10, 2009

ABSTRACT

The biological role of quadruplexes and polyamines has been independently associated with cancer. However, quadruplex-polyamine mediated transcriptional regulation remain unaddressed. Herein, using c-*MYC* quadruplex model, we have attempted to understand quadruplex–polyamine interaction and its role in transcriptional regulation. We initially employed biophysical approach involving CD, UV and FRET to understand the role of polyamines (spermidine and spermine) on conformation, stability, molecular recognition of quadruplex and to investigate the effect of polyamines on quadruplex–Watson Crick duplex transition. Our study demonstrates that polyamines affect the c-*MYC* quadruplex conformation, perturb its recognition properties and delays duplex formation. The relative free energy difference ($\Delta\Delta G^{\circ}$) between the duplex and quadruplex structure indicate that polyamines stabilize and favor c-*MYC* quadruplex over duplex. Further, we investigated the influence of polyamine mediated perturbation of this equilibrium on c-*MYC* expression. Our results suggest that polyamines induce structural transition of c-*MYC* quadruplex to a transcriptionally active motif with distinctive molecular recognition property, which drives c-*MYC* expression. These findings may allow exploiting quadruplex–polyamines interaction for developing antiproliferative strategies to combat aberrant gene expression.

INTRODUCTION

Polyamines are ubiquitous low molecular weight aliphatic cations, which are involved in a large number of cellular processes including functioning of ion channels, nucleic acid packaging, DNA replication, apoptosis, transcription and translation (1–5). These multivalent cations also act as electrostatic bridges between the phosphate charges of DNA and RNA as well as a variety of other highly charged linear chains, e.g. filaments and microtubules. Cells have evolved mechanisms to ensure the tight regulation of intracellular polyamine pools. The total intracellular concentration of polyamines is in millimolar range. However, the free polyamine concentrations are considerably lower, as they are bound to anionic groups in DNA, RNA, proteins and phospholipids (6–8). Insufficient levels of polyamines result in suboptimal growth and high levels of polyamines can lead to malignant transformation (9,10). The naturally occurring polyamines include putrescine, spermidine and spermine, which are involved in signal transduction. Different polyamines preferentially activate protein kinases (tyrosine kinases and MAP kinases), which accelerate the expression of nuclear proto-oncogenes (11–14). One of such proto-oncogenes codes for a nuclear transcription factor c-MYC, which play a central role in the regulation of cell cycle progression. Polyamine-induced nuclear c-MYC interacts with MAX, and this complex binds to E-box sequence CAC GTG to activate transcription of target genes. The enzyme ornithine decarboxylase (ODC) involved in polyamine biosynthesis harbors two conserved CACGT G elements. MYC–MAX complex activates ODC by binding to these elements, thus accelerating polyamine biosynthesis (15–17).

The transcriptional regulation of c-*MYC* gene is complex, and involves multiple promoters (P0, P1 and P2) (17). The nuclease hypersensitivity element (NHE III) upstream of P1 promoter controls c-*MYC* transcription and has been a subject of considerable research over the past few decades (18). The NHE III of c-*MYC* region contains pyrimidine-rich coding strand and a purine-rich noncoding strand. The purine (guanine)-rich strand can adopt intramolecular fold back structure called G-quadruplexes, which contains a planar array of G-quartets paired by Hoogsteen bonds (19). Such guanine-rich sequences are also found in other promoter elements (*VEGF*, c-*KIT* and *BCL2*, etc.), telomeres, centromeres, immunoglobulin switch regions and mutational

*To whom correspondence should be addressed. Tel: +91 11 2766 6156; Fax: +91 11 2766 7471; Email: souvik@igib.res.in, souvik2maiti@yahoo.com

hot spot regions (19–21). Recently, a genome-wide search has shown as many as 376 000 potential quadruplexes could exist in the functionally important regions of genes (22,23). The increasing evidence of quadruplexes being implicated in disease has kindled interest in developing synthetic ligands that can bind selectively to these structures, affect their molecular recognition properties, which allows exploiting them as therapeutic target (24,25). However, the potential existence of these structures is relevant only if they are investigated in presence of other competing structures. In the genome, the guanine stretches are present along with their C-rich complementary strand, which generates competition between Hoogsteen-bonded quadruplex structure and Watson–Crick hydrogen-bonded duplex structure. The structural transition amongst these secondary structures may in turn modulate the gene function. This quadruplex–duplex competition is influenced by pH, temperature, salt concentration and complementary strand concentration (26–35). We have previously reported the influence of natural (molecular crowding) and pharmacological (cationic porhyrin) agent on quadruplex–duplex equilibrium, these perturbants stabilize the quadruplex and shift the equilibrium to quadruplex formation (33).

Quadruplexes are implicated in cancer (19–21) and an increase in cellular polyamines concentration leads to cancer progression (9,10). This suggests the existence of an elemental link between these two independent events, which may mutually result in oncogenesis. Herein, we attempt to establish an association between these phenomena using c-*MYC* quadruplex as a model. The target sequence used in this study is a 22-mer purine-rich sequence of NHE III of *c-MYC* promoter located from –143 to –110 bp upstream of P1 promoter. It has been shown that there is a facile transformation of this purine-rich sequence of the NHE III in the c-*MYC* promoter to a kinetically favored parallel G-quadruplex that acts as a transcriptional switch in gene expression (18). We adopted biophysical approach Circular Dichroism (CD), Ultraviolet (UV) and Fluorescence Resonance Energy Transfer (FRET) to understand the role of polyamines (spermidine and spermine) in influencing the conformation, stability, molecular recognition of quadruplex and quadruplex–Watson Crick transition. Our study demonstrates that polyamines affect the conformation of c-*MYC* quadruplex, modulates its molecular recognition and delays hybridization to its complementary strand for duplex formation. This modulation of molecular recognition of c-*MYC* quadruplex in the promoter consequently affects the downstream c-*MYC* expression. This work provides insight into role of polyamines–quadruplex interaction that may affect probable biological function of quadruplexes and lead to disease condition.

MATERIALS AND METHODS

Oligonucleotides

Single-labeled (5′-fluorescein) and dual-labeled (5′-fluorescein and 3′-TAMRA) sequence d(GGGGAGGGTGG GGAGGGTGGGG) were obtained from Microsynth. Unlabeled G-rich and C-rich strands were obtained from Sigma. All the oligonucleotides were High Performance Liquid Chromatography (HPLC) purified. The concentrations of unlabeled oligonucleotides were calculated by extrapolation of tabulated values of the monomer bases and dimers at 25°C using procedures reported earlier (36,37).

CD study

CD spectrum of c-*MYC* 22-mer quadruplex (5 μM) was recorded using a Jasco 715 spectropolarimeter at 25°C. The sample was prepared by slow annealing in 10 mM sodium cacodylate buffer, pH 7.4 and 100 mM NaCl and 100 mM KCl. Spectra were recorded with increasing concentrations of spermidine (0–0.75 mM) and spermine (0–50 μM) in NaCl and KCl buffers. Duplex sample was prepared by heating mixture of G-rich (5 μM) and its C-rich complementary strand (50 μM) in 10 mM Tris buffer, pH 7.4 at 95°C, followed by slow cooling. The duplex samples (5 μM) were incubated with 0.75 mM spermidine and 50 μM spermine for 3 h in 10 mM Tris buffer, pH 7.4 at 25°C and CD spectra were recorded from 200 nm to 350 nm.

Nondenaturing gel electrophoresis

Quadruplex was prepared using 5′-fluorescein-GGGGAG GGTGGGGAGGGTGGGG-3′ by heating at 95°C, followed by slow annealing in 100 mM NaCl. Preformed quadruplex (2 μM) was incubated with 0.75 mM spermidine and 50 μM spermine for 3 h in 10 mM sodium cacodylate buffer pH 7.4, 100 mM NaCl at 25°C. Duplex sample was prepared by heating the mixture of G-rich (1.5 μM) and its C-rich complementary strand (30 μM) in 10 mM Tris buffer, pH 7.4 at 95°C, followed by slow cooling. The duplex samples (2 μM) were incubated with 0.75 mM spermidine and 50 μM spermine for 3 h in 10 mM Tris buffer, pH 7.4 at 25°C. All the samples were electrophoresed on 15% polyacrylamide nondenaturing gel and gel was run in 1× Tris borate EDTA (TBE), pH 7.4 at 4°C at constant voltage of 100 V. The gel was visualized in Fujifilm phosphorimager using 480 nm laser and 520 nm filter. Gel experiment was also performed using nonquadruplex-forming sequences and their respective duplex in the absence and presence of polyamines (0.75 mM spermidine and 50 μM spermine). The sequences used were: Sequence 1: 5′-GCTTGCTTCCTTCG-3′ and Sequence 2: 5′-CGAAGGAAGCAAGC-3′. The samples of 5 μM concentration were prepared in 10 mM Tris buffer, pH 7.4 for T_{15} marker, single strand and duplex. All the samples were electrophoresed on 15% polyacrylamide nondenaturing gel and gel was run in 1× TBE, pH 7.4 at 4°C at constant voltage of 100 V. After electrophoresis, gel was stained with ethidium bromide and was visualized through BioRad Gel Doc XR.

UV melting study

c-*MYC* quadruplex sample was prepared by heating the oligonucleotides in 10 mM sodium cacodylate buffer, pH 7.4, 100 mM NaCl and 100 mM KCl followed by slow cooling. The melting profile of c-*MYC* quadruplex

(2 μM) was recorded in absence and presence of 0.75 mM spermidine and 5 μM spermine in Cary 100 (Varian) spectrophotometer equipped with Hitachi SPR-10 thermoprogrammer with a heating/cooling rate of 0.2°C/min and data were collected at 295 nm. T_m was calculated from the peak value of the first derivative of the absorbance profile. Thermodynamic parameters were determined using method reported previously (38). We also performed concentration-dependent UV experiments (2 μM to 75 μM) to check concentration-independent melting temperature for unstructured–structured transition to differentiate between intra- and intermolecular system.

UV–vis absorption titration study

Absorption spectra were measured on a Cary100 UV–vis spectrophotometer with a 1-cm path length quartz cell. UV–vis absorption titrations were carried out by the stepwise addition of quadruplex solution to a cell containing 1.0 μM TMPyP4 (porphyrin) and absorption spectra were recorded in the 350–550 nm range at 25°C. The experiments were performed in 10 mM sodium cacodylate buffer, pH 7.4, 100 mM NaCl and 100 mM KCl. The data were analyzed with both single- and double-binding models using Equations (1) and (2), respectively, as described previously (47).

$$r = (n_1 \times C_f)/(K_d \times C_f) \quad \mathbf{1}$$

$$r = (n_1 \times C_f)/(K_{d1} + C_f) + (n_2 \times C_f)/(K_{d2} + C_f) \quad \mathbf{2}$$

where r is the number of moles of TMPyP4 bound to 1 mol of G-quadruplex, n_1 and n_2 are the stoichiometries of TMPyP4-quadruplex interaction, C_f is the free TMPyP4 concentration and K_{d1} and K_{d2} are the quadruplex–TMPyP4 equilibrium dissociation constants. Origin 7.0 was used for all the fitting analysis.

Fluorescence study

FRET experiments were performed using sequence 5′ fluorescein-GGGGAGGGTGGGGAGGGTGGGG-3′ TAMRA and data were recorded in Nanodrop fluorospectrometer (ND-3330). The samples were prepared with fixed concentration of preformed quadruplex (0.15 μM) and with increasing concentrations of complementary strand (0–30 μM) and incubated for 24 h at 25°C. The experiment was performed in the absence and presence of 0.75 mM spermidine and 50 μM spermine in 10 mM sodium cacodylate buffer, pH 7.4, 100 mM NaCl and 100 mM KCl. Data were analyzed for fluorescein signal at 520 nm as reported previously (27).

Kinetic experiments were also performed in fluorospectrometer (ND-3300). The solution containing equimolar concentrations (0.15 μM) of preformed quadruplex and its complementary strand were prepared in the absence and presence of 0.75 mM spermidine and 50 μM spermine in 10 mM sodium cacodylate buffer, pH 7.4, 100 mM NaCl at 25°C and aliquots of samples were read at different time intervals. The fluorescence signal of fluorescein at 520 nm was fitted to mono-exponential kinetic equation to obtain hybridization kinetics for duplex formation.

Fluorescence-annealing experiments were performed in LC 480 (Roche). The annealing profile of the equimolar mixture of quadruplex (0.15 μM) and its complementary strand in the absence and presence of spermidine (0.75 mM) and spermine (50 μM) in 10 mM sodium cacodylate buffer, pH 7.4, 100 mM NaCl was recorded with a cooling rate of 0.2°C/min. Normalized Donor (fluorescein) emission ($I_{520\,nm} = F_t/F_{95}$) at 520 nm was plotted as a function of temperature, where F_t is the fluorescence of donor at any temperature and F_{95} is the fluorescence of donor at 95°C.

RNA isolation and real time Polymerase Chain Reaction (PCR)

Exponentially growing 1×10^6 HeLa cells in Dulbecco's Modified Eagle Medium (DMEM) media supplemented with 10% Fetal Calf Serum (FCS) were seeded in six-well plate on Day 1. The cells were treated with different concentrations of spermidine (0–15 mM) and spermine (0–15 mM) on Day 2. After 24 h of polyamines treatment, cells were lysed for RNA isolation. In another experiment to investigate the influence of polyamines on the efficacy of quadruplex-interacting ligand TMPyP4 (porphyrin), the cells were given pre-treatment of spermidine (15 mM) and spermine (15 mM) on Day 1. On Day 2, the media was changed and cells were treated with different concentrations of porphyrin (0–30 μM). The control sample included cells, which were not given any polyamine or porphyrin treatment. After 24 h of porphyrin treatment, the cells were lysed using Trizol reagent (Invitrogen) (39). The Trizol reagent (1 ml) was added in a six-well plate and continuous pipetting was done for 5 min. After homogenization, 200 μl of chloroform was added to the samples followed by vortexing for 30 s and incubation at room temperature for 5 min. The samples were then centrifuged at 12 000 r.p.m. for 15 min at 4°C and the obtained aqueous phase was transferred to fresh tube. Isopropanol (500 μl) was added in the samples and these were incubated at −20°C for 60 min. The samples were again centrifuged at 12 000 r.p.m. for 15 min at 4°C and followed by 2 washes by 70% ethanol and centrifugation. The pellet was air dried and dissolved in 20 μl of double autoclaved MQ water. Quantification of RNA was done using Nanodrop (ND-1000) spectrometer. The samples were then given DNase I treatment to remove DNA contamination and RNA quality was checked by running a 1.5% agarose gel. cDNA was synthesized using High Capacity kit (ABI) as per manufacture's protocol. cDNA quality was checked by performing PCR with respective primers and observing the desired band for PCR product. This was followed by real time PCR in LC 480 (Roche) using SYBER green master mix as per manufacture's protocol to assess the transcript level of target gene (c-*MYC*) with respect to internal reference genes *B2m* and β-*actin*. Data analysis was done to obtain fold change by Pafflʼs method (51). The primers used for real time PCR were: c-*MYC* primers (forward primer: TGAGGAGACACCG CCCAC; reverse primer: CAACATCGATTTCTTCCTC

ATCTTC); *B2m* primers (forward primer: TGCTGTCTC CATGTTTGATGTATCT, reverse primer: TCTCTGCT CCCCACCTCTAAGT) and β-*actin* primers (forward primer: AAGAGAGGCATCCTCACCCT, reverse primer: TACATGGCTGGGGTGTTGAA).

Transfection and luciferase assay

Exponentially growing 1×10^6 HeLa cells in DMEM media supplemented with 10% FCS were seeded in a six-well plate on Day 1. The plasmids used for transfection were Del 4 which harbors the 22-mer c-*MYC* quadruplex-forming sequence in the P1 promoter upstream of the luciferase reporter (a gift from Bert Vogelstein) and Del 4 mutant plasmids that had substitutions in the quadruplex-forming sequence, which destabilizes the structure (a gift from Shantanu Chowdhury) (40). The quadruplex-forming sequences upstream of luciferase reporter gene in the plasmids used in the current study are following: Del 4: 5′-GGGGAGGGTGGGGAGGGTGGGG-3′; Mut 1: 5′-GGGGAGGGTGAGGAGGGTGGGG-3′ and Mut 2: 5′-GGGGAGGGTGAAGAGAGTGGGG-3′, where substitutions are underlined. One microgram plasmid was transfected in HeLa cells growing at 75% confluency using Lipofectamine 2000 as per manufacture's protocol. After 5 h of transfection, the cells were given 1× PBS wash and fresh media was added in each well and cells were given subsequent polyamines (0–15 mM spermidine and spermine) treatment for 24 h. The cells were lysed with 1× Cell Culture Lysis Reagent (CCLR) buffer (Promega Luciferase Assay System Cat no #E1500) with continuous pipetting at 4°C for 30 min. The homogenate was centrifuged for 2 min at 10 000*g*. The supernatant is used for protein estimation by Bicinchoninic Acid (BCA) method. Luciferase assay was performed in Orion Microplate Luminometer (Berthold Detection System) for three biological replicates and luciferase activity was normalized by total protein concentration.

RESULTS AND DISCUSSION

The CD spectrum recorded for 22-mer purine-rich sequence of NHE III of c-*MYC* promoter in 100 mM NaCl buffer depicts an intense positive peak at 265 nm, a small positive peak at 295 nm and a negative peak at 240 nm, thus suggesting the existence of a predominant parallel quadruplex population along with a small antiparallel population (Figure 1). The increasing concentrations of polyamines (0–0.75 mM spermidine and 0–50 μM spermine) lead to a prominent increase in the magnitude of positive peak at 265 nm and a moderate increase in the negative peak at 240 nm with a concomitant decrease in the magnitude of positive peak at 295 nm. This suggests that polyamines induce structural transitions which result in decrease in antiparallel population and a simultaneous increase in parallel population. Similar experiments were performed in KCl buffer, and only a moderate effect for the structural transition from antiparallel to parallel conformation was observed (Supplementary Figure 1). In KCl buffer, c-*MYC* quadruplex displays very high thermal stability (T_m = 75°C, Supplementary Figure 3) and this

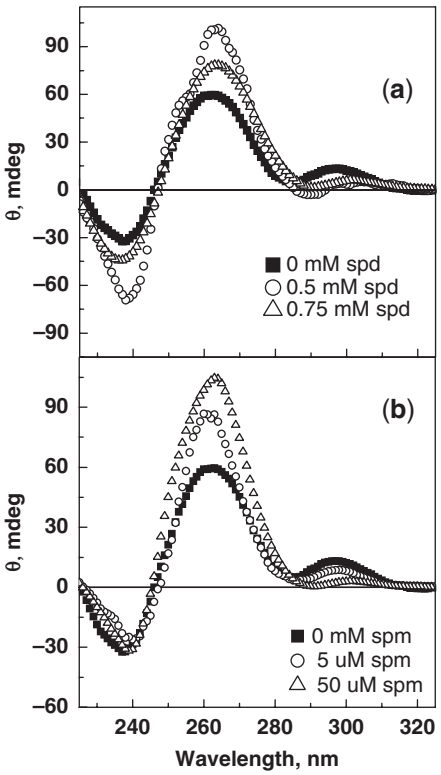

Figure 1. CD spectra recorded for c-*MYC* quadruplex (5 μM) in absence and presence of (**a**) spermidine and (**b**) spermine in 10 mM sodium cacodylate buffer, 100 mM NaCl, pH 7.4 at 25°C.

structure might resist the induction of any further structural transitions by polyamines. A further increase in concentration of spermidine (>0.75 mM) and spermine (>50 μM) resulted in precipitation of DNA both in NaCl and KCl buffers. Therefore, the working concentration was restricted to 0–0.75 mM spermidine and 0–50 μM spermine in our subsequent experiments. Since, this 22-mer G-rich sequence has potential to adopt more than one conformation, the difference in their mobility would allow resolving these populations through native gel electrophoresis. We performed native gel electrophoresis to observe the structural transitions induced by polyamines, as shown in Figure 2 (lanes 2–4). The presence of two discrete bands for quadruplex signifies existence of mixed conformers in NaCl buffer, and is in concordance with our CD observations. However, in presence of both 0.75 mM spermidine and 50 μM spermine, we observed decrease in the intensity of lower band and an increase in the intensity of upper band suggesting the shift towards one type of conformer, probably the parallel population as observed in the CD study.

For quadruplex formation, G-rich regions must be released from the duplex DNA, which hints towards the existence of an interconversion between intramolecular quadruplex and intermolecular Watson–Crick duplex structure for execution of various cellular processes like replication, recombination, transcription, etc. The 22-mer G-rich element used in this study belongs to the NHE III region of c-*MYC* gene, and it adopts intramolecular

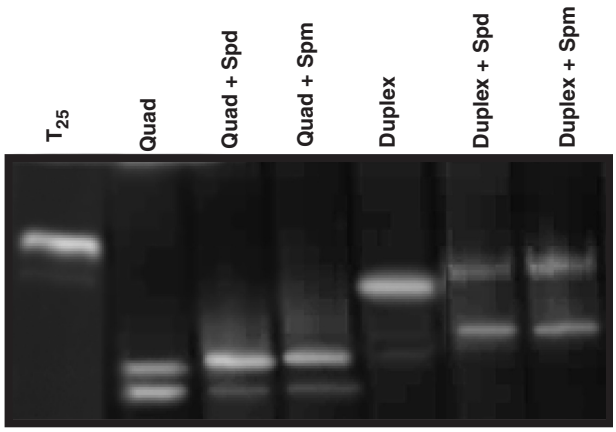

Figure 2. Native gel electrophoresis of fluorescein-labeled quadruplex. Lane 1 represents oligo T_{25}; lanes 2–4 represent quadruplex (2 μM) in absence and presence of 0.75 mM spermidine (Spd) and 50 μM spermine (Spm), respectively; lanes 5–7 represent duplex (2 μM) in absence and presence of 0.75 mM spermidine and 50 μM spermine, respectively.

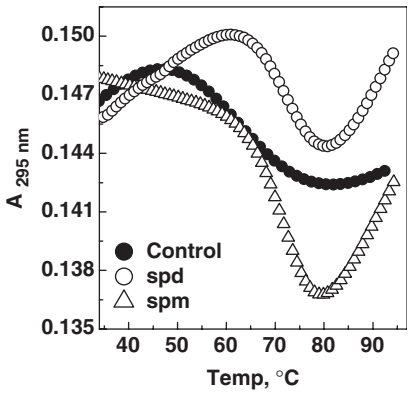

Figure 3. UV melting profile of c-*MYC* quadruplex (2 μM) in absence and presence of 0.75 mM spermidine and 50 μM spermine in 10 mM sodium cacodylate buffer, 100 mM NaCl, pH 7.4.

secondary structure, which may control multiple rounds of transcription before it switches back to the usual B-DNA conformer. However, during the onset of cancerous condition, intracellular concentration of polyamines increases, which may affect the nucleic acid structures and their dynamic transitions between interconverting alternative secondary structures. As polyamines stabilize quadruplex structure and induce structural transition to predominant one type of conformer, they might also influence the hybridization of the G-rich structured strand to its complementary strand and thereby, modulate the structural transition between usual Watson–Crick duplex and quadruplex structure. We used native gel electrophoresis to monitor the effect of polyamines on duplex formation and to resolve the quadruplex and duplex populations. Duplex DNA in the absence of polyamines gave a sharp single band thereby suggesting presence of predominant duplex population. However, in presence of polyamines, we observed emergence of an extra band with higher mobility, which corresponded to quadruplex formation, thereby suggesting structural transition from the usual Watson–Crick duplex to unusual quadruplex structure (Figure 2, lanes 5–7). We also confirmed these results through CD experiment under similar conditions (Supplementary Figure 4). The CD spectrum of duplex in absence of polyamines exhibits a positive peak at 278 nm and negative peak at 250 nm. However, in presence of polyamines we observe a broad peak at 274 nm and a negative peak at 242 nm. The shoulder peak at 262 nm signifies the contribution of the induced quadruplex population. Thus, both gel and CD study show that polyamines drive structural transition from duplex to quadruplex. We also performed gel study to monitor the influence of polyamines on the mobility of a nonquadruplex-forming sequence and its duplex. The data show that polyamines does not have any effect on the mobility of both single-stranded oligonucleotides and their corresponding duplex (Supplementary Figure 5).

Next, we evaluated the effect of polyamines on the thermal stability of c-*MYC* quadruplex by monitoring the melting profile at 295 nm. The thermal melting was observed to be independent of quadruplex concentration both in absence and presence of polyamines, thereby suggesting formation of intramolecular structure (Supplementary Figure 2). The UV melting profile shows that this element forms a stable quadruplex with T_m of 62.5°C in 100 mM NaCl buffer. The increase in the concentration of spermidine (0–0.75 mM) and spermine (0–50 μM) resulted in increase in the stability of quadruplex structure. The maximum increase in thermal stability was obtained at 0.75 mM spermidine and 50 μM spermine with T_m of 71.5°C and 70°C, respectively (Figure 3 and Table 1). The enthalpy change associated with quadruplex melting was −24.3 kcal/mol in absence of polyamines, −54.0 kcal/mol and −67.0 kcal/mol in presence of 0.75 mM spermidine and 50 μM spermine, respectively. Similar experiments were also performed in potassium buffer. Quadruplex formed in potassium buffer is highly stable (T_m = 75°C, Supplementary Figure 3), but in presence of polyamines we did not obtain characteristic melting domain, as c-*MYC* quadruplex–K^+ in presence of polyamines melts at temperatures >90°C (Supplementary Figure 3). Through UV melting study, it is difficult to dissect out the contributions from the participating populations: quadruplex, duplex and random coil. Therefore, we performed fluorescence-annealing experiments to understand the contribution of these populations and comprehend the fate of equilibrium (30,34). Annealing the system slowly from 95°C to 37°C containing both the G-rich and its complementary strand generates a competing environment that allows the G-rich oligonucleotide to either exist as quadruplex and/or hybridize to its complementary strand to form duplex depending on relative thermodynamic stabilities of these two secondary structures. We monitored the annealing profile of donor fluorescence intensity at 520 nm for c-*MYC* G-rich sequence with equimolar concentration of complementary strand in the absence and presence of polyamines (Figure 4). The annealing profile obtained for the equimolar mixture of G-rich and C-rich strand in absence of polyamines, initially showed a marginal decrease in fluorescence intensity upon decrease in temperatures from 95°C to 76°C. But at ~76°C, a change in fluorescence

Table 1. Thermodynamic parameters obtained from UV and fluorescence experiments performed in 10 mM sodium cacodylate buffer, 100 mM NaCl, pH 7.4 at 25°C

	Quad[a]			Duplex[b]			
	T_m (°C)	ΔH° (kcal/mol)	$\Delta G^\circ_{25}{}^{quad}$ (kcal/mol)	τ_{25} (h)	K_A ($10^6\,M^{-1}$)	$\Delta G^\circ_{25}{}^{duplex}$ (kcal/mol)	$\Delta\Delta G^\circ_{25}$ (kcal/mol)
Quad	62.5	−24.30 (±0.80)	−2.60 (±0.35)	5.20 (±0.5)	3.30 (±0.2)	−8.86	−6.25
Quad + 0.75 mM spermidine	71.5	−53.0 (±0.70)	−7.11 (±0.22)	9.20 (±0.6)	0.56 (±0.4)	−7.81	−0.70
Quad + 50 μM spermine	70.0	−67.00 (±0.56)	−7.40 (±0.78)	10.70 (±0.8)	0.36 (±0.6)	−7.55	−0.14

[a]UV experiments were performed with 1 μM quadruplex concentration. T_m values are within ±0.5°C error.
[b]Fluorescence experiments were performed with dual labeled (5′-fluorescein and 3′-TAMRA) preformed quadruplex (0.15 μM concentration). τ_{25} is time constant for duplex formation, K_A is binding affinity for duplex formation. ΔG°_{25} was determined using the relation $\Delta G^\circ = -RT \ln K_A$, where R is universal gas constant, T is temperature. $\Delta\Delta G^\circ$ is relative free energy difference between duplex and quadruplex.

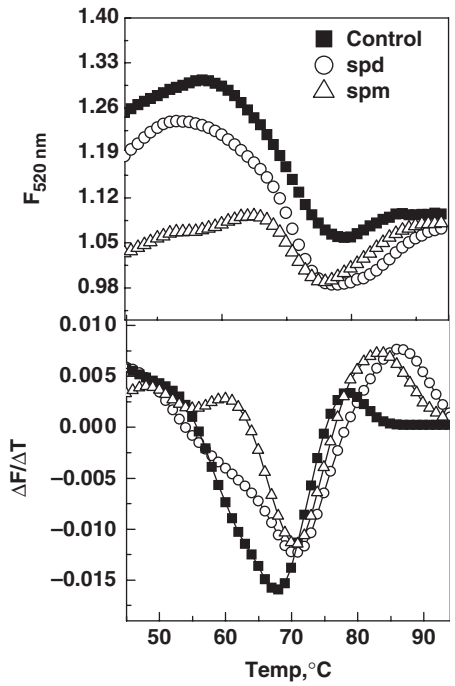

Figure 4. Fluorescence-annealing curves obtained for equimolar mixture of quadruplex (0.15 μM) and its complementary strand in absence and presence of 0.75 mM spermidine and 50 μM spermine in 10 mM sodium cacodylate buffer, 100 mM NaCl, pH 7.4.

profile was observed which showed increase in fluorescence with further decrease in temperature (76–37°C). The initial decrease and subsequent increase in fluorescence in the cooling profile corresponds to quadruplex and duplex formation, respectively. The fluorescence intensity change at different temperatures is reflective of these contributing populations. The fluorescence profile of donor intensity monitored for the equimolar mixture of G-rich and C-rich strand in presence of 0.75 mM spermidine and 50 μM spermine shows a prominent decrease in fluorescence intensity upon decrease in temperature from 95°C to 76°C and the profile shifts to higher temperature, as shown in Figure 4. Upon further decrease in temperature (76–37°C), the fluorescence intensity increased indicating duplex formation. The extent of increase in fluorescence intensity of donor is lesser in presence of polyamines, suggesting lesser amount duplex formation in comparison to absence of polyamines. The first derivative of these melting curves shows two peaks corresponding to quadruplex and duplex melting domains at higher and lower temperatures, respectively. The intensity and peak position of derivative curve reflect the amount of each participating population and their corresponding T_m values (34). We observed only a moderate shift in the duplex melting domain to higher temperatures in presence of polyamines. However, a prominent shift of quadruplex melting domain to higher temperatures was observed. This can be attributed to the competing secondary structures, quadruplex and duplex adopted by the G-rich sequence. Polyamine-induced stabilization of quadruplex facilitates greater quadruplex formation, and results in decrease in effective G-rich strands required for duplex formation, leading to a marginal increase in duplex stability in presence of polyamines. Polyamines show remarkable stabilizing effects on DNA–RNA hybrids, stem-loop structures and triplexes (41,42). Numerous studies have shown that polyamines interact with DNA anionic phosphate backbone, condense the DNA and induce B–Z transitions. More direct evidences have been obtained by NMR studies, which support the existence of nonspecific electrostatic interactions between DNA backbone and cationic polyamines. These studies also revealed that association of polyamines with B-DNA is weak, whereas their association with the folded quadruplex structure is stronger (43,44). Literature findings suggest that high affinity of polyamines toward non-B-DNA secondary structures is governed by both secondary structure and its base composition (45,46).

Next, we investigated the role of polyamines on the thermodynamics and kinetics of duplex formation. We determined the binding affinity of the preformed quadruplex to its complementary strand in absence and presence of the 0.75 mM spermidine and 50 μM spermine. We observed the binding affinity of c-*MYC* quadruplex to its complementary structure in absence of polyamine was $3.3 \times 10^6\,M^{-1}$. However, in presence of 0.75 mM spermidine and 50 μM spermine the binding affinity reduced by an order to $3.6 \times 10^5\,M^{-1}$ and $5.6 \times 10^5\,M^{-1}$, respectively (Figure 5, Table 1). We also investigated the kinetics

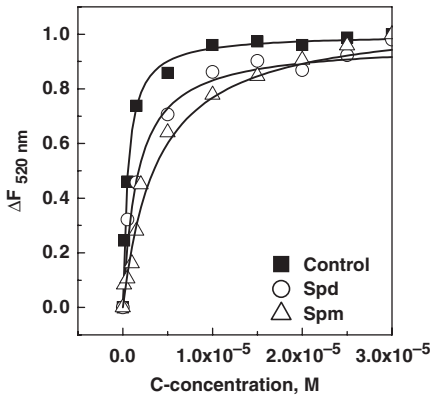

Figure 5. Normalized fluorescence of quadruplex (0.15 μM) at 520 nm as a function of complementary strand concentrations in absence and presence of 0.75 mM spermidine and 50 μM of spermine in 10 mM sodium cacodylate buffer, 100 mM NaCl, pH 7.4 at 25°C.

of hybridization of preformed quadruplex to its complementary strand in absence and presence of polyamines. The fluorescence change was fit to single exponential fit with good residuals. The time constant obtained for hybridization in absence of polyamines was 5.2 h. However, in presence of 0.75 mM spermidine and 50 μM sperimine the time constant for duplex formation doubled (Table 1 and Supplementary Figure 6). To check the interference of polyamines on fluorescence properties of fluorophore, we also recorded the spectra of fluorescein-labeled C-rich strand in absence and at experimental concentrations of polyamines. As observed in Supplementary Figure 7, the fluorescence spectra were similar in absence and presence of polyamines. Similar experiments were also performed in KCl buffer; however, as quadruplex is extremely stable in KCl buffer, and polyamines further stabilize this structure, it becomes difficult to extract thermodynamic and kinetic parameters with reasonable accuracy. Risitano and Fox (30) have shown that the sequence from c-*MYC* promoter preferentially adopts quadruplex structure in potassium-containing buffers and requires the presence of 50-fold excess of complementary strand for duplex formation. As hybridization of preformed c-*MYC* quadruplex–K^+ suffers from thermodynamic and kinetic barrier, the presence of polyamines would further hinder the association between the two strands in potassium buffers. Our biophysical experiments indicate that c-*MYC* quadruplex under physiological conditions is stable and predominates in quadruplex–Watson–Crick duplex equilibrium in both sodium and potassium buffers. The important parameter that would dictate the predominance of either of the population (duplex or quadruplex) is the relative free energy difference, the $\Delta\Delta G^\circ$ between duplex and quadruplex structure. $\Delta\Delta G^\circ$ obtained under experimental conditions was −6.25 kcal/mol, −0.70 kcal/mol and −0.14 kcal/mol in the absence, presence of 0.75 mM spermidine and 50 μM spermine, respectively. The significant decrease in the magnitude of $\Delta\Delta G^\circ$ in presence of polyamines highlights the prominent contribution from competing quadruplex structure. Polyamines induce structural transition to one type of conformer in c-*MYC* quadruplex, stabilize this structure and delay its hybridization to its complementary strand. We have reported similar observations for delay in hybridization of telomeric quadruplex to its complementary strand in presence of natural and pharmacological agents (33).

Since quadruplexes are involved in molecular recognition and function, polyamines-induced structural changes increase the predominance of a particular conformer over another, and consequently affect recognition by the protein/ligand. To investigate this, we assessed the binding affinity of a pharmacological agent (cationic porphyrin, TMPyP4) to quadruplex in absence and presence of polyamines. Binding of TMPyP4 to c-*MYC* quadruplex resulted in ~76% hypochromicity and 20 nm bathochromic shift of peak at 421 nm (Supplementary Figure 8). These spectral changes of porphyrin obtained upon titration with quadruplex are indicative of intercalative mode of binding. This is in agreement with a recent study that demonstrated two binding modes for c-*MYC* quadruplex–TMPyP4 interaction using spectroscopic and calorimetric techniques (47,48). In presence of 0.75 mM spermidine and 50 μM spermine, the hypochromicities obtained were 72% and 68%, respectively. Data analysis showed that the c-*MYC* quadruplex has two independent sites with different binding affinity for porphyrin (Figure 6). In absence of polyamines, porphyrin binds to c-*MYC* quadruplex at these independent sites with a binding affinity of 2.6 $(\pm 0.4) \times 10^8\,M^{-1}$ and 1.5 $(\pm 0.3) \times 10^6\,M^{-1}$. In presence of 0.75 mM spermidine, the binding affinity obtained for porphyrin binding to quadruplex was 2.0 $(\pm 0.5) \times 10^7\,M^{-1}$ and 2.4 $(\pm 0.3) \times 10^5\,M^{-1}$. Similar observations were obtained in 50 μM of spermine, where the binding affinity obtained for this interaction was 2.5 $(\pm 0.2) \times 10^7\,M^{-1}$ and 7.6 $(\pm 0.3) \times 10^5\,M^{-1}$. We also determined the binding affinity for quadruplex–porphyrin in presence of polyamines in KCl buffer. In the absence of polyamines, porphyrin binds to independent sites with binding affinity of 1.5 $(\pm 0.4) \times 10^7\,M^{-1}$ and 1.0 $(\pm 0.5) \times 10^6\,M^{-1}$ in KCl buffer. In presence of polyamines, porphyrin binding significantly reduces by one order for both the binding sites. The binding affinity obtained was 4.0 $(\pm 0.2) \times 10^6\,M^{-1}$ and 3.5 $(\pm 0.6) \times 10^5\,M^{-1}$ in 0.75 mM spermidine, and 3.5 $(\pm 0.5) \times 10^6\,M^{-1}$ and 2.0 $(\pm 0.6) \times 10^5\,M^{-1}$ in 50 μM spermine, respectively, in KCl buffer (Supplementary Figure 9). The binding sites showed an order decrease in binding affinity for quadruplex–porphyrin interaction in both NaCl and KCl buffers, hence suggesting the critical role of polyamines in modulating the molecular recognition and interaction with binding partners. This explains the observed ineffectiveness of quadruplex-interacting pharmacological agents in cancer, which demonstrate promising *in vitro* results.

The interesting biophysical observations prompted us to perform molecular assay to extrapolate the findings of polyamines-induced structural transition, stabilization and modulation of molecular recognition properties of c-*MYC* quadruplex structure to c-*MYC* transcription. Literature cites independent observations of both quadruplex and increased polyamine concentrations being involved in uncontrolled cellular proliferation. This hints

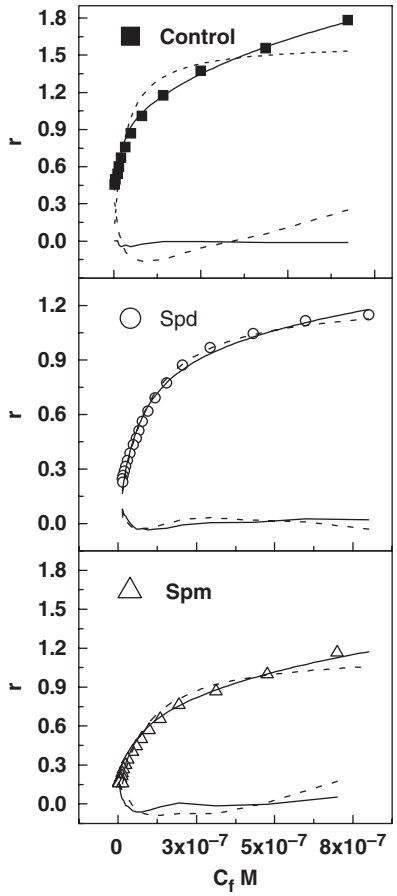

Figure 6. Binding data analysis for quadruplex–porphyrin (TMPyP4) interaction in absence (filled square) and presence (open circle) of 0.75 mM sperimidine and (open triangle) 50 μM spermine in10 mM sodium cacodylate buffer, 100 mM NaCl, pH 7.4 at 25°C. The *y*-axis represents *r* (moles of bound TMPyP4/1 mol of quadruplex) and *x*-axis represents C_f, which is concentration of free TMPyP4. Data analysis was performed using one-site and two-site hyperbolic equations. Fitting data and its residuals are shown for one-site (dash) and two-site binding (solid) for the quadruplex–porphyrin interaction.

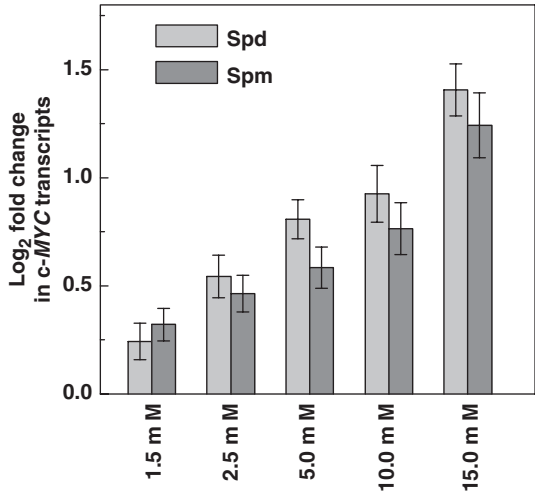

Figure 7. Fold change in the c-*MYC* transcripts assessed through real time PCR after 24 h of treatment of polyamines (0–15 mM spermidine and spermine) to HeLa cells. The fold change represents the $\log_2$-fold change of c-*MYC* transcripts with respect to internal reference gene for treated samples versus control sample, which received no polyamine treatment. Expression level of *B2m* gene was taken as internal reference gene to normalize the real time PCR data. The data represent the mean values ± SDs from three separate experiments.

toward the existence of an underlying phenomenon, which may associate physical interaction between quadruplex and intracellular polyamines to ensue cancer progression. The aberrant gene expression observed during cancer progression can be attributed to modulation of molecular recognition, physical interaction and function of nucleic acid structures upon interaction with polyamines. c-*MYC* is an important proto-oncogene which is involved in growth differentiation of cells and regulation of other proto-oncogenes (15,17). The aberrant expression of c-*MYC* is associated with broad range of cancers. Further, the quadruplex element in the promoter region of c-*MYC* proto-oncogene is structurally and functionally well characterized, and this motif is believed to play a role in c-*MYC* expression (18,49). We have previously established that quadruplex–duplex equilibrium has important role in modulating gene expression (50). As quadruplex in c-*MYC* promoter serves as a structural target for gene regulation, any perturbation in quadruplex–duplex equilibrium induced by polyamines would affect downstream c-*MYC* expression. To ascertain this belief, we assessed c-*MYC* transcript levels in absence and presence of polyamines in cell culture system. We performed real time PCR experiment to analyze the relative changes in c-*MYC* gene expression with respect to the internal reference gene. c-*MYC* transcript levels were assessed after treating the cells with increasing concentrations (0–15 mM) of spermidine and spermine and data were analyzed by mathematical model for relative quantification of target (c-*MYC*) versus internal reference gene (*B2m*) expression (51). We obtained a concentration-dependent increase in c-*MYC* transcript levels upon treating the cells with increasing concentrations (0–15 mM) of spermidine and spermine (Figure 7). These experiments were also performed using β-*actin* gene as internal reference gene. It is noteworthy to mention that β-*actin* harbors the quadruplex forming sequence potential in its promoter region, whereas *B2m* lacks this potential in its promoter. Interestingly, polyamine does not significantly affect the gene expression of both *B2m* and β-*actin* genes, thereby resulting in similar trend in c-*MYC* activation (Figure 7 and Supplementary Figure 10). Polyamine interaction with this c-*MYC* quadruplex motif affects its stability, molecular recognition and induces structural transition into a transcriptionally active conformer, which drives c-*MYC* activation. This implies that the quadruplex–polyamine interaction will translate into molecular consequences, where the quadruplex in the promoter region serves as functional regulatory motif and controls the expression of the downstream gene.

We were also interested in investigating whether polyamines can interfere with the efficacious response of the quadruplex-interacting ligand. We assessed the transcriptional activity of c-*MYC* gene upon treatment of cells with

porphyrin (TMPyP4) and data shows a dose-dependent decrease in c-*MYC* transcript levels (Supplementary figure 11A) which is in agreement with the previous reports (18,40). However, a pre-treatment of polyamines (spermidine and spermine) followed by porphyrin treatment does not lead to significant transcriptional suppression of c-*MYC* gene (Supplementary Figure 11B). Although porphyrin is also associated with nonspecific effects (48), the observed ineffective biological response of promising quadruplex-interacting ligands is due to the induced structural transition and perturbation of molecular recognition of DNA structures by small molecules in cancerous condition.

Quadruplex has been previously demonstrated as a repressor element (18). However, recent genome-wide analysis of regulatory role of quadruplex motifs reveal quadruplex-mediated stimulation of transcription (52). Quadruplex formation allows maintenance of open chromatin state and facilitates multiple rounds of transcription. This is supported by new reports where the activator role of c-*MYC* quadruplex (50) and dual role (activator and repressor) for c-*MYB* has been demonstrated (53). We observed that both polyamines and porphyrin (TMPyP4) stabilize quadruplex but mediate different biological consequence of c-*MYC* transcription. Polyamines induce structural transition of c-*MYC* quadruplex to a transcriptionally active motif with distinctive molecular recognition property for transcription factor binding, which drives c-*MYC* expression. On the other hand, porphyrin (TMPyP4) binding to c-*MYC* quadruplex does not induce any structural change in quadruplex conformation (54,55); however, it masks or competes with the transcription factor binding leading to c-*MYC* downregulation. Studies have shown that promoter regions harboring G-quadruplex potential have binding sites for one or more transcription factors (53). These protein factors may compete for same or exclusive binding sites. As a consequence, the co-existence of events of secondary structure formation and protein–DNA interaction may influence each other to either activate or repress gene expression. Therefore, our observation is in concordance with growing body of evidences where quadruplexes have been associated with both activator and repressor roles (20,50,52,53,56,57).

To further affirm that the observed c-*MYC* activation is governed by quadruplex–polyamine interaction, we performed reporter assay using plasmids having native target c-*MYC* quadruplex-forming sequence (Del 4) and its mutated sequence (Mut 1 and Mut 2) in the promoter upstream of reporter luciferase gene ('Materials and Methods' section). We observed that increase in polyamine (0–15 mM spermidine and spermine) concentration induces increase in luciferase activity in the cells transfected with these plasmids. This increment in reporter activity was more pronounced in Del 4 plasmid as compared to the mutated plasmids, which harbored mutation in the quadruplex forming sequence that destabilized the quadruplex motif (Supplementary Figure 12). Polyamines exhibit stabilizing effects on mutated quadruplex motifs also, but are able to drive only moderate increase in reporter activity. However, in case of the native sequence, polyamines induce remarkable stabilization and structural transition to a transcriptionally active motif, which drives increased luciferase reporter expression. In the current experiment, the complete truncation of the quadruplex-forming sequence would result in loss of reporter activity as the sequence harbors protein factor binding sites; therefore, we restricted the study to native and mutated sequence harboring plasmids. In summary, our results from the real time PCR and reporter assays convincingly emphasize the importance quadruplex–polyamine interaction-mediated perturbation of c-*MYC* expression.

Polyamines have influence on chromatin structure (7,8), and numerous studies have demonstrated that changes in chromatin structure modulates c-*MYC* expression (15,17,18). Previous literature reports have shown the molecular associations of polyamines with other proto-oncogenes like c-*JUN*, c-*FOS*, *NF-κB* and tumor suppressor genes like *p*53 and *Rb* (9–12). Recently, it has been identified that these genes harbor the potential of quadruplex-forming regulatory elements in the promoter region and these structures are believed to serve as recognition motifs, which modulate the downstream gene expression (22,23). Taken together the literature evidences and our current observations suggest that quadruplex–polyamine interaction perturbs the transcription of genes that are under the transcriptional control of quadruplex motif and not for genes having the mere existence of quadruplex-forming sequence in its promoter region. Our biophysical and molecular observations provide an explanation to the literature evidences, which discernibly establish that polyamines stimulate c-*MYC* expression. Polyamines cause structural transition and stabilization of parallel conformer and delay its hybridization to its complementary strand. This conformer displays distinctive molecular recognition property, which might fabricate it into more transcriptionally active motif to drive aberrant c-*MYC* expression.

CONCLUSION

The study emphasizes the role of aliphatic cations like spermidine and spermine in affecting the quadruplex conformation, stability and molecular recognition by a pharmacological agent. These aliphatic cations also perturb the dynamic equilibrium between the multistranded structure and Watson–Crick duplex structure, and consequently affect the gene expression by trapping quadruplex in transcriptionally active conformer. With both quadruplexes and polyamines being implicated in cancer, a thorough understanding of polyamine and nucleic acid structure interaction would reinforce the interest in adopting strategy for antiproliferation, which would interfere in polyamine–quadruplex interaction.

SUPPLEMENTARY DATA

Supplementary Data is available at NAR Online.

ACKNOWLEDGEMENTS

N.K. acknowledges CSIR for fellowship and S.M. acknowledges CSIR for funding this research. We thank Bert Vogelstein for providing Del 4 and Shantanu Chowdhury for providing Mut 1 and Mut 2 plasmids. We also thank the anonymous referees for critical inputs, which helped us to improve the manuscript.

FUNDING

Council of Scientific and Industrial Research (CSIR). Open Access Publication charges were waived by Oxford University Press.

Conflict of interest statement. None declared.

REFERENCES

1. Cohen,S.S. (1998) *A Guide to the Polyamines*. New York, Oxford University Press.
2. Pendeville,H., Carpino,N., Marine,J.C., Takahashi,Y., Muller,M., Martial,J.A. and Cleveland,J.L. (2001) The ornithine decarboxylase gene is essential for cell survival during early murine development. *Mol. Cell Biol.*, **21**, 6549–6558.
3. Williams,K. (1997) Interactions of polyamines with ion channels. *Biochem. J.*, **325**, 289–297.
4. Xie,X., Tome,M.E. and Gerner,E.W. (1997) Loss of intracellular putrescine pool-size regulation induces apoptosis. *Exp. Cell Res.*, **230**, 386–392.
5. Ruan,H., Hill,J.R., Fatemie-Nainie,S. and Morris,D.R. (1994) Cell-specific translational regulation of S-adenosylmethionine decarboxylase mRNA. Influence of the structure of the 5′ transcript leader on regulation by the upstream open reading frame. *J. Biol. Chem.*, **269**, 17905–17910.
6. Bachrach,U., Wang,Y.C. and Tabib,A. (2001) Polyamines: new cues in cellular signal transduction. *News Physiol Sci.*, **16**, 106–109.
7. D'Agostino,L. and Di Luccia,A. (2002) Polyamines interact with DNA as molecular aggregates. *Eur. J. Biochem.*, **269**, 4317–4325.
8. Ha,H.C., Yager,J.D., Woster,P.A. and Casero,R.A. Jr. (1998) Structural specificity of polyamines and polyamine analogues in the protection of DNA from strand breaks induced by reactive oxygen species. *Biochem. Biophys. Res. Commun.*, **244**, 298–303.
9. Tabib,A. and Bachrach,U. (1998) Polyamines induce malignant transformation in cultured NIH 3T3 fibroblasts. *Int. J. Biochem. Cell Biol.*, **30**, 135–146.
10. Thomas,T. and Thomas,T.J. (2003) Polyamines metabolism and cancer. *J. Cell Mol. Med.*, **7**, 113–126.
11. Khosravi-Far,R. and Der,C.J. (1994) The Ras signal transduction pathway. *Cancer Metastasis Rev.*, **13**, 67–89.
12. Tabib,A. and Bachrach,U. (1994) Activation of the proto-oncogenes c-*myc* and c*fos* by c-*ras*: involvement of polyamines. *Biochem. Biophys. Res. Commun.*, **202**, 720–727.
13. Ray,R.M., Bhattacharya,S. and Johnson,L.R. (2007) EGFR plays a pivotal role in the regulation of polyamine-dependent apoptosis in intestinal epithelial cells. *Cell Signal.*, **19**, 2519–2527.
14. Kutuzov,M.A., Andreeva,A.V. and Voyno-Yasenetskaya,T.A. (2005) Regulation of apoptosis signal-regulating kinase 1 (ASK1) by polyamine levels via protein phosphatase 5. *J. Biol. Chem.*, **280**, 25388–25395.
15. Pelengaris,S., Khan,M. and Evan,G. (2002) c-MYC: more than just a matter of life and death. *Nat. Rev. Cancer*, **2**, 764–776.
16. Patel,A.R. and Wang,J.Y. (1997) Polyamines modulate transcription but not posttranscription of c-myc and c-jun in IEC-6 cells. *Am. J. Physiol. Cell Physiol.*, **273**, C1020–C1029.
17. Marcu,K.B., Bossone,S.A. and Patel,A.J. (1992) myc function and regulation. *Annu. Rev. Biochem.*, **61**, 809–860.
18. Siddiqui-Jain,A., Grand,C.L., Bearss,D.J. and Hurley,L.H. (2002) Direct evidence for a G-quadruplex in a promoter region and its targeting with a small molecule to repress c-MYC transcription. *Proc. Natl. Acad. Sci. USA*, **99**, 11593–11598.
19. Ghosal,G. and Muniyappa,K. (2006) Hoogsteen base-pairing revisited: resolving a role in normal biological processes and human diseases. *Biochem. Biophys. Res. Commun.*, **343**, 1–7.
20. Maizels,N. (2006) Dynamic roles for G4 DNA in the biology of eukaryotic cells. *Nat. Struct. Mol. Biol.*, **13**, 1055–1059.
21. Fry,M. (2007) Tetraplex DNA and its interacting proteins. *Front. Biosci.*, **12**, 4336–4351.
22. Huppert,J.L. and Balasubramanian,S. (2005) Prevalence of quadruplexes in the human genome. *Nucleic Acids Res.*, **33**, 2908–2916.
23. Todd,A.K., Johnston,M. and Neidle,S. (2005) Highly prevalent putative quadruplex sequence motifs in human DNA. *Nucleic Acids Res.*, **33**, 2901–2907.
24. Hurley,L.H., Wheelhouse,R.T., Sun,D., Kerwin,S.M., Salazar,M., Fedoroff,O.Y., Han,F.X., Han,H., Izbicka,E. and Von Hoff,D.D. (2002) G-quadruplexes as targets for drug design. *Pharmacol. Ther.*, **85**, 141–158.
25. Izbicka,E., Wheelhouse,R.T., Raymond,E., Davidson,K.K., Lawrence,R.A., Sun,D., Windle,B.E., Hurley,L.H. and Von Hoff,D.D. (1999) Effects of cationic porphyrins as G-quadruplex interactive agents in human tumor cells. *Cancer Res.*, **59**, 639–644.
26. Deng,H. and Braunlin,W.H. (1995) Duplex to quadruplex equilibrium of the self-complementary oligonucleotide d(GGGGCCCC). *Biopolymers*, **35**, 677–681.
27. Kumar,N. and Maiti,S. (2004) Quadruplex to Watson-Crick duplex transition of the thrombin binding aptamer: a fluorescence resonance energy transfer study. *Biochem. Biophys. Res. Commun.*, **319**, 759–767.
28. Phan,A.T. and Mergny,J.L. (2002) Human telomeric DNA: G-quadruplex, i-motif and Watson–Crick double helix. *Nucleic Acids Res.*, **30**, 4618–4625.
29. Li,W., Wu,P., Ohmichia,T. and Sugimotoa,N. (2002) Characterization and thermodynamic properties of quadruplex/duplex competition. *FEBS Lett.*, **526**, 77–81.
30. Risitano,A. and Fox,K.R. (2003) Stability of intramolecular DNA quadruplexes: comparison with DNA duplexes. *Biochemistry*, **42**, 6507–6513.
31. Kumar,N. and Maiti,S. (2007) Role of locked nucleic acid modified complementary strand in quadruplex/Watson-Crick duplex equilibrium. *J. Phys. Chem. B.*, **111**, 12328–12337.
32. Li,W., Miyoshi,D., Nakano,S. and Sugimoto,N. (2003) Competition involving G-quadruplex DNA and its complement. *Biochemistry*, **42**, 11736–11744.
33. Kumar,N. and Maiti,S. (2005) The effect of osmolytes and small molecule on quadruplex–WC duplex equilibrium: a fluorescence resonance energy transfer study. *Nucleic Acid Res.*, **33**, 6723–6732.
34. Rachwal,P.A. and Fox,K.R. (2007) Quadruplex melting. *Methods*, **43**, 291–301.
35. Kumar,N., Sahoo,B., Varun,K.A.S., Maiti,S. and Maiti,S. (2008) Effect of loop length variation on quadruplex-duplex competition. *Nucleic Acid Res.*, **36**, 4433–4442.
36. Cantor,C.R., Warshaw,M.M. and Shapiro,H. (1970) Oligonucleotide interactions. 3. Circular dichroism studies of the conformation of deoxyoligonucleotides. *Biopolymers*, **9**, 1059–1077.
37. Marky,L.A., Blumenfeld,K.S., Kozlowski,S. and Breslauer,K.J. (1983) Salt-dependent conformational transitions in the self-complementary deoxydodecanucleotide d(CGCAATTCGCG): evidence for hairpin formation. *Biopolymers*, **9**, 1247–1257.
38. Kumar,N. and Maiti,S. (2008) A thermodynamic overview of naturally occurring intramolecular DNA quadruplexes. *Nucleic Acids Res.*, **36**, 5610–5622.
39. Chomczynski,P. and Sacchi,N. (2006) The single-step method of RNA isolation by acid guanidinium thiocyanate-phenol-chloroform extraction: twenty-something years on. *Nat. Protoc.*, **1**, 581–585.
40. Thakur,R.K., Kumar,P., Halder,K., Verma,A., Kar,A., Parent,J.L., Basundra,R., Kumar,A. and Chowdhury,S. (2009) Metastases suppressor NM23-H2 interaction with G-quadruplex DNA within c-MYC promoter nuclease hypersensitive element induces c-MYC expression. *Nucleic Acid Res.*, **37**, 172–183.
41. Thomas,T. and Thomas,T.J. (1993) Selectivity of polyamines in triplex DNA stabilization. *Biochemistry*, **32**, 14068–14074.

42. Antony,T., Thomas,T., Shirahata,A., Sigal,L.H. and Thomas,T.J. (1999) Selectivity of spermine homologs on triplex DNA stabilization. *Antisense Nucleic Acid Drug Dev.*, **9**, 221–231.
43. Keniry,M.A. (2003) A comparison of the association of spermine with duplex and quadruplex DNA by NMR. *FEBS Lett.*, **542**, 153–158.
44. Keniry,M.A. and Owen,E.A. (2007) An investigation of the dynamics of spermine bound to duplex and quadruplex DNA by (13)C NMR spectroscopy. *Eur. Biophys. J.*, **36**, 637–646.
45. Anderson,W.H., Braunlin,C.F. and Record,M.T. (1986) ^{23}Na-NMR investigations of counterion exchange reactions of helical DNA. *Biopolymers*, **25**, 205–214.
46. Manning,G.S. (1979) Counterion binding in polyelectrolyte theory. *Acc. Chem. Res.*, **12**, 443–449.
47. Arora,A. and Maiti,S. (2008) Effect of loop orientation on quadruplex-TMPyP4 interaction. *J. Phys. Chem. B*, **112**, 8151–8159.
48. Anantha,N.V., Azam,M. and Sheardy,R.D. (1998) Porphyrin binding to quadrupled T4G4. *Biochemistry*, **37**, 2709–2714.
49. Phan,A.T., Modi,Y.S. and Patel,D.J. (2004) Propeller-type parallel-stranded G-quadruplexes in the human *c-myc* promoter. *J. Am. Chem. Soc.*, **126**, 8710–8716.
50. Kumar,N., Patowary,A., Sivasubbu,S., Petersen,M. and Maiti,S. (2008) Silencing c-*MYC* expression by targeting quadruplex in P1 promoter using locked nucleic acid based trap. *Biochemistry*, **47**, 13179–13188.
51. Pfaffl,M.W. (2001) A mathematical model for relative quantification in real-time RT-PCR. *Nucleic Acids Res.*, **29**, e45.
52. Du,Z., Zhao,Y. and Li,N. (2008) Genome-wide analysis reveals regulatory role of G4 DNA in gene transcription. *Genome Res.*, **18**, 233–241.
53. Palumbo,S.L., Memmott,R.M., Uribe,D.J., Krotova-Khan,Y., Hurley,L.H. and Ebbinghaus,S.W. (2008) A novel G-quadruplex-forming GGA repeat region in the c-myb promoter is a critical regulator of promoter activity. *Nucleic Acid Res.*, **36**, 1755–1769.
54. Seenisamy,J., Rezler,E.M., Powell,T.J., Tye,D., Gokhale,V., Joshi,C.S., Siddiqui-Jain,A. and Hurley,L.H. (2004) The dynamic character of the G-quadruplex element in the c-MYC promoter and modification by TMPyP4. *J. Am. Chem. Soc.*, **126**, 8702–8709.
55. Freyer,M.W., Buscaglia,R., Kaplan,K., Cashman,D., Hurley,L.H. and Lewis,E.A. (2007) Biophysical studies of the c-MYC NHE III1 promoter: model quadruplex interactions with a cationic porphyrin. *Biophys. J.*, **92**, 2007–2015.
56. Verma,A., Halder,K., Halder,R., Yadav,V.K., Rawal,P., Thakur,R.K., Mohd,F., Sharma,A. and Chowdhury,S. (2008) Genome-wide computational and expression analyses reveal G-quadruplex DNA motifs as conserved cis-regulatory elements in human and related species. *J. Med. Chem.*, **51**, 5641–5649.
57. Verma,A., Yadav,V.K., Basundra,R., Kumar,A. and Chowdhury,S. (2009) Evidence of genome-wide G4 DNA-mediated gene expression in human cancer cells. *Nucleic Acids Res.*, doi:10.1093/nar/gkn1076.